Hydrodynamic characteristics of aquiferous modules in the demosponge Halichondria panicea

Kealy, Rachael A.; Busk, Thomas; Goldstein, Josephine; Larsen, Poul S.; Riisgård, Hans Ulrik

Published in:
Marine Biology Research

Link to article, DOI:
10.1080/17451000.2019.1694691

Publication date:
2019

Document Version
Peer reviewed version

Hydrodynamic characteristics of aquiferous modules in the demosponge *Halichondria panicea*

Rachael A. Kealy[1], Thomas Busk[1], Josephine Goldstein[1], Poul S. Larsen[2], Hans Ulrik Riisgård[1*]

[1]Marine Biological Research Centre, University of Southern Denmark, Hindsholmvej 11, DK-5300 Kerteminde, Denmark
[2]DTU Mechanical Engineering, Fluid Mechanics, Technical University of Denmark, Building 403, DK-2800 Kgs. Lyngby, Denmark

[*]Corresponding author

Abstract: Multi-oscula sponges are organisms composed of aquiferous modules, each of which draws water through its canal system by means of pumping units (choanocyte chambers, *CC*) such that the filtered water leaves the module as an exhalant jet through the osculum of the module. Here we compare relations between the characteristic parameters of sponge volume (V), osculum cross-sectional area (OSA), exhalant jet speed (U_0), and filtration rate (F) of single-osculum explants and individual aquiferous modules of multi-oscula explants of the demosponge *Halichondria panicea*. The latter modules are identified by observing from which part of the surface administered dye will emerge from its osculum. There is fair agreement in results between the two types of modules. For both types, the filtration rate is a linear function of the modules volume, with average values of volume-specific filtration rate of 1.8 and 1.5 ml min^{-1} cm^{-3} for single- and multi-oscula sponge explants, respectively. This supports the hypothesis that the density of *CC*s is approximately constant for a given species. Although the individual modules in a multi-oscula sponge operate as separate aquiferous systems, the present study has shown that modules nevertheless communicate in response to external stimuli. Thus, when one module was exposed locally to ink particles, both the exposed module and its neighbouring modules reduced their OSA, U_0, and F.

Keywords: Exhalant jet speed; Filtration rate; Osculum area; Scaling; Aquiferous module; Contraction

---

Introduction

Sponges (Porifera) are among the oldest groups of multicellular organisms in the animal kingdom (Metazoa) with fossil records dating back to over 700 million years (Brian et al. 2012) They are comprised of at least eight cell types and the entire body is specialized for filter-feeding on suspended organic particles (i.e. free-living bacteria and phytoplankton) in the ambient water (Jørgensen 1966; Reiswig 1971, 1974, 1975; Bergquist 1978; Simpson 1984; Larsen and Riisgård 1994; Elliott and Leys 2007; Leys et al. 2011; Ludeman et al. 2014; Strehlow et al. 2016; Lüskow et al. 2018). Sponges lack nerves and muscles, but have muscle-like cells (myocytes) resembling smooth muscle cells which, along with chemical messenger-based systems enable sponges to react to environmental stimuli in a coordinated way of contraction-inflation behavior (Parker 1910; Bagby 1966; Perovic et al. 1999; Nickel 2004, 2011; Nickel et al. 2006; Elliott and Leys 2007, 2010; Ellwanger et al. 2007; Ludeman et al. 2014; Leys 2015).

Sponges are modular organisms in which each "aquiferous module" is a functional unit that draws ambient water through numerous small inhalant openings (ostia) into an inhalant canal system by means of pumping units (choanocyte chambers, *CC*). These

*CC*s filter the water for bacteria, phytoplankton and other suspended food particles before the water leaves the module via an exhalant canal system through a single exhalant opening (osculum) to the surrounding water (Fry 1970, 1979; Ereskovskii 2003). In a recent study, Goldstein et al. (2019) stated that a constant density of *CC*s in sponges would imply that the theoretical scaling of sponge volume (V_s), osculum cross-sectional area (*OSA*), exhalant jet speed (U_0), and filtration rate (F) could be expressed as $OSA \sim V_s^{2/3}$, $U_0 \sim OSA^{1/2}$ and $F \sim OSA^{3/2}$. Experimental data obtained on single-osculum sponge explants (i.e. single aquiferous modules) of the demosponge *Halichondria panicea* Pallas, 1766 showed that the observed scaling with size was close to that inferred from the hypothesis of constant *CC* density (Goldstein et al. 2019). Thus, the increase of U_0 with increasing *OSA* may be expressed by a power function with an exponent of 0.5 and (based on literature data, Goldstein et al. 2019, Fig. 10 therein) reach a maximum value of U_0 = 6 to 8 cm s^{-1}. This suggests that U_0 approaches an upper limit which in turn implies that a sponge module of the species in question may increase only to a certain size.

According to Fry (1970, 1975) the development of an osculum may be in response to expel drawn in water from a certain volume of sponge, referred to as an aquiferous module. Thus, a multi-oscula sponge may be regarded as a "population of aquiferous modules" (Fry 1970). Because the size of the *OSA* seems to be closely correlated with both sponge volume and filtration rate it has been of interest in the present study to determine the size of individual modules and their filtration rate in both single-osculum and multi-oscula sponge explants. Although the aquiferous systems of the individual modules in a multi-oscular sponge are separate functional units this may not exclude - communication between modules leading to coordinated oscular contractions triggered by inorganic particles, and therefore it has been of interest to study the effect of inorganic particle overloading in multi-oscula sponges.

Materials & Methods

Sponges were sourced from larger colonies of the demosponge *Halichondria panicea* at the inlet to Kerteminde Fjord, Denmark (55°26'59"N, 10°39'40"E) and transported to the Marine Biological Research Centre laboratory. Small cuttings ranging from 0.03 to 1.68 cm^3 were placed on glass slides in temperature-controlled (16.1±0.9 °C) flow-through aquaria with bio-filtered (blue mussels, *Mytilus edulis* Linneaus, 1758) seawater (23.0±0.9 PSU). Development of a single osculum (or several oscula) was regularly monitored. In addition, multi-oscula explants were produced from larger sponge fragments with several oscula and were attached to substrate plates with whipping twine. All explants were kept in flow-through aquaria and fed lab-cultured *Rhodomonas salina* Wislouch, Hill and Wetherbee, 1989 algal cells (~5000 cells ml^{-1}) for 6 h every 1 to 3 days.

Osculum diameter (D, mm) of the aquiferous modules in explants were measured video-microscopically using the software ImageJ v5.0.3 to determine the osculum cross-sectional area (*OSA*, mm^2) as:

$$OSA = \pi(D/2)^2 \quad . \qquad \text{Eq. (1)}$$

To serve as a reference, the oscula of 69 sponges were photographed *in situ* in the inlet to Kerteminde Fjord 4 October 2018 to determine the size distribution of *OSA* in the field. For single-osculum explants, i.e. individual aquiferous modules, the side-view projected area (A, mm^2) and height (h, mm), were measured for volume estimates (V_{est}, mm^3) using the cone equation (Goldstein et al. 2019):

$$V_{est} = \pi A^2/3h \quad . \qquad \text{Eq. (2)}$$

For multi-oscula explants, the boarders of aquiferous modules were identified through observations of incurrent and excurrent water flow using fluorescence. Fluorescein dye (20 PSU, 12°C) was deposited on the exopinacoderm in small doses (~0.1 ml) using a micromanipulator. The micromanipulator was repositioned over the sponge explant (distance from explants ~0.5 mm) to determine where fluorescein stopped exiting one osculum and began exiting another. Exhalant jets were visualized with fluorescein dye while all oscula were open to ensure water flow through the entire sponge. The volume of each aquiferous module in a multi-oscula explant was directly measured (V_{mea}, mm³) by cutting along the invisible boarders of an aquiferous module and weighing each module individually. Comparative volume estimates (V_{est}, mm³) were obtained based on the relative contribution of each aquiferous module to the total volume flow through the entire explant, based on the hypothesis that volume-specific filtration rate is constant and the same for all modules, leading to the equation:

$$V_{est} = F_{est}/\sum F_{est} \times \sum V_{mea} \quad , \qquad \text{Eq. (3)}$$

where F_{est} is the estimated filtration rate of each aquiferous module, $\sum F_{est}$ (ml min^{-1}) the total filtration rate and $\sum V_{mea}$ the total measured volume of the multi-oscula explant.

The flow speed of the exhalant jet near expanded oscula of aquiferous modules was estimated from the motion of ink particles smaller than 6 µm (Pelikan Scribtol; dilution 2×10^5-fold to give an estimated particle density of 10^4 ml^{-1}). High-speed (60.61 fps) video recordings (duration 100 s) of the particle movement in a focal (side view) plane near the exhalant jet were analysed by particle tracking velocimetry (PTV; Goldstein et al. 2019) using the software IC Capture 2.3. The exhalant jet speed (U_0), defined as the mean velocity at the osculum, was determined by extrapolating the velocity of moving particles to the osculum using exponential regression (Goldstein et al. 2019). The filtration rate of each aquiferous module was estimated from the osculum cross-sectional area and the exhalant jet speed using the following equation:

$$F_{est} = OSA \times U_0 \quad . \qquad \text{Eq. (4)}$$

A comparative measure of the filtration rate was obtained for a single-osculum explant using the clearance method (Riisgård et al. 2016) during simultaneous determination of *OSA* and U_0. The clearance method is based on the exponential decrease in algal (*R. salina*) concentration (C, cells ml^{-1}) caused by a sponge explant over time. Since sponges retain *R. salina* cells of mean diameter 6.3 µm with 100 % efficiency (Jørgensen 1966; Bergquist 1978), the clearance rate is equal to the filtration rate (= pumping rate). Prior to experimentation, the explant was placed in bio-filtered seawater (V = 400 ml) with constant mixing for 1 h to minimise effects of external stimuli. Algal cells (*R. salina*) were added in an average concentration <5000 cells ml^{-1} and samples (10 ml) were taken at fixed time intervals (15 min) to measure the algal concentration using an electronic particle counter (Elzone 5380). Samples were returned to the experimental tank after each measurement to avoid significant reduction in seawater volume. The filtration rate (F_{mea}, ml min^{-1}) was calculated from the slope (b, min^{-1}) of the regression line in a semi-ln plot for the decrease in algal concentration over time and the volume (V, ml) of seawater in the experimental tank (Riisgård et al. 2016):

$$F_{mea} = V \times b \quad . \qquad \text{Eq. (5)}$$

Coordination among aquiferous modules in multi-oscula explants was explored by exposing individual modules to ~2 ml (100-fold diluted stock) of inorganic (ink) particles and simultaneously monitoring the exhalant jet speed.

Statistical analyses

Statistical data analyses were performed in R version 3.1.3 (R Core Team 2015). Linear models (LM) were parameterized to determine the decrease in algal concentration (C) in a semi-ln plot over time, to extrapolate the velocity field of moving particles to the osculum ($x = 0$) using exponential regression and for fitting power functions to the relationships between osculum cross-sectional area (OSA) and module volume (V_{est} or V_{mea}, respectively), jet speed (U_0) and OSA, or filtration rate (F_{est}) and OSA. Generalized mixed-effect models (GLMM) with Gamma error structure were parameterized to test for differences in OSA, U_0 or F_{est} between undisturbed and ink-exposed multi-oscula explants (fixed effect) by correcting for individual variation (random effect).

Results

Single-osculum sponge explants

From a total number of 70 single-osculum *Halichondria panicea* explant cuttings, 63 % attached to substrate plates after 3±3 days, and 69 % had developed one or more oscula after 6±4 days. The average volume (V) of explant cuttings with a single osculum (osculum cross-sectional area $OSA = 0.5\pm0.3$ mm^2) was $V = 0.5\pm0.4$ ml ($n = 31$) and the average volume of explant cuttings with more than one osculum ($OSA = 1.2\pm0.7$ mm^2) was $V = 0.6\pm0.4$ ml ($n = 14$). The obtained data for 17 single-osculum explants of various size, including the osculum cross-sectional area (OSA), estimated explant volume (V_{est}), exhalant jet speeds (U_0) and estimated filtration rates (F_{est}) is shown in Table 1. The OSA of single-osculum explants increased significantly as a function of V_{est} (LM, $t_{0.21, 15} = 2.8$, $P = 0.012$), following a power function with an exponent of 0.38 (Fig. 1). Both U_0 and F_{est} were positively correlated with OSA (Fig. 2). U_0 increased as a function of OSA with a power exponent of 0.57 (LM, $t_{0.23, 15} = 2.5$, $P = 0.026$), reaching an upper limit of about 25 mm s^{-1} in the OSA range 0.2 to 1.1 mm^2 (Fig. 2A). F_{est} increased with increasing OSA following a power exponent of 1.26 (Fig. 2B; LM, $t_{0.15, 14} = 7.8$, $P = 1.8\times10^{-6}$). Direct measurement of the filtration rate of a single-osculum *H. panicea* explant ($V = 1.0$ cm³) using Eq. (5) was $F_{mea} = (0.009$ min$^{-1}\times400$ ml$) = 3.6$ ml min^{-1} (Fig. 3; LM, $t_{0.08, 5} = -9.3$, $P = 2.4\times10^{-4}$) was in good agreement with a simultaneous mean estimate of the filtration rate $F_{est} = 2.7\pm0.8$ ml min^{-1} obtained via particle tracking velocimetry (Table 2). The volume-specific filtration rates (F_V) of the single-osculum sponges are shown in Table 1, and the mean (±S.D.) rate was estimated at 1.8±1.0 ml min^{-1} cm^{-3}.

Multi-oscula sponge explants

The water flow through multi-oscula *Halichondria panicea* explants is laminar, as reflected by the thin exhalant jet visualized by fluorescein dye added locally to the exterior sponge body of a single aquiferous module (Fig. 4). The total volume of multi-oscula explants was 0.7 to 4.2 ml, of which aquiferous modules constituted independent volumes of 0.1 to 3.7 ml (Table 3). The average volume of individual aquiferous modules in multi-oscula explants was 1.1±1.0 ml. The average size of an *OSA in situ* was 1.0±0.6 mm^2 from a size range of 0.2 to 3.1 mm^2 (Fig. 5), which shows that laboratory samples were of a representative size. In the laboratory studies, occasional contractions of oscula were observed, but all reported results are for expanded oscula. The observed OSA of undisturbed aquiferous modules ranged from 0.1 to 3.1 mm^2 and exhalant jet speeds of up to 57.2 mm s^{-1} were measured (Table 3). Corresponding

estimated filtration rates were in the range 0.1 to 6.2 ml min^{-1} for individual aquiferous modules and reached up to 9.4 ml min^{-1} for an entire multi-oscula explant (Table 3). *OSA* of aquiferous modules increased with increasing aquiferous module volume (V_{mea}), following a power function with exponent 1.01 (Fig. 6; LM, $t_{0.20, 12} = 8.2$, $P = 3.01\times10^{-6}$). U_0 of aquiferous modules increased with *OSA* to an exponent of 0.29 (Fig. 7A; LM, $t_{0.31, 12} = 1.7$, $P = 0.11$), in fair agreement with the exponent (0.38) obtained for single-osculum explants (Fig. 1). A power exponent of 1.06, close to that (1.26) for single-osculum explants, was observed for the relationship F_{est} *versus OSA* in multi-oscula explants (Fig. 7B; LM, $t_{0.25, 12} = 7.62$, $P = 6.18\times10^{-6}$).

Exposing a single aquiferous module to ink particles caused contractile behaviour in the exposed and in most neighbouring modules of the multi-oscula explants (Table 3). Induced contractile behaviour was expressed by significantly reduced *OSA*s (GLMM, $t_{0.27, 11} = -2.6$, $P = 0.011$), and in some cases, additional reductions in U_0 (GLMM, $t_{1.11, 12} = -2.5$, $P = 0.803$), thus causing severe decreases in F_{est} (GLMM, $t_{0.47, 12} = -2.7$, $P = 0.006$) of the entire explants when compared to undisturbed conditions (Table 3).

The volume-specific filtration rate of the modules in 6 multi-oscula sponges are shown in Table 3, and the mean (±S.D.) was $F_V = 1.5\pm0.6$ ml min^{-1} cm^{-3}, close to that (1.8 ml min^{-1} cm^{-3}) obtained for single osculum explants (Table 1).

Discussion

Single-osculum sponge explants

For the single-osculum explants the three exponents (0.38, 0.57 and 1.26) in the power-law correlations of Figs. 1, 2A and 2B deviate from those (2/3, 1/2 and 3/2) expected according to the theoretical scaling (Goldstein et al. 2019). Here, the exponent (0.38) in the power-law correlations of *OSA versus* V_{est} in Figs. 1 is significantly smaller than 2/3. As a consequence, the exponent (1.26) in the correlation for F_{est} *versus OSA* (Fig. 2B) also takes a low value (< 3/2) because the exponent (0.57) for U_0 *versus OSA* (Fig. 2A) is close to the expected value (1/2), and because of the dependence $F_{est} = U_0\times OSA$. The present *OSA* range (0.2 to 1.1 mm^2) is less than that (0.1 to 3.1 mm^2) of Goldstein et al. (2019) which showed exponents (0.66, 0.45 and 1.45) of power-law correlations that are in better agreement with the theoretical scaling. However, considering only the narrower *OSA* range (0.2 to 1.1 mm^2) in that study leads also to low values of exponents (0.56, 0.30 and 1.31), indicating a trend similar to the present. The volume-specific filtration rate of the present explants (1.8±1.0 ml min^{-1} cm^{-3}) is lower and shows less variation than that (3.46 ±3.25 ml min^{-1} cm^{-3}) observed by Goldstein et al. (2019), but values are of the same order of magnitude which supports the hypothesis that the density of choanocyte pumping units may be approximately constant for a given species. Also, there appears to be no size effect since the subset of values for *OSA* range 0.2 to 1.1 mm^2 gives similar results (3.64±3.44 ml min^{-1} cm^{-3}).

Multi-oscula sponge explants

For multi-oscula sponge explant aquiferous modules the three exponents (1.01, 0.29 and 1.06) in the power-law correlations of Figs. 6, 7A and 7B may be compared with those (2/3, 1/2 and 3/2) expected according to the theoretical scaling (Goldstein et al. 2019), and those (0.38, 0.57 and 1.26) of the present single-osculum explants. The observed deviations from the expected exponents may partly be explained by different ranges of *OSA*-values. Thus, the range of *OSA* was small, 0.2 to 1.1 mm^2 for single-osculum explants while it was about 3 times larger, 0.1 to 3.1 mm^2 for multi-oscula explants resulting in exponents in better agreement with the theoretical ones.

For individual aquiferous modules (of mean volume 0.86 ml, Table 3) the mean volume-specific filtration rate (1.5±0.6 ml min^{-1} cm^{-3}) is slightly less than that (1.8±1.0

ml min^{-1} cm^{-3}, Table 1) of the present single-osculum explants (of mean volume 0.35 ml). Further, these values may be compared to 3.2 ml min^{-1} cm^{-3} for single-osculum explants of *Halichondria panicea* studied by Goldstein et al. (2019) (Fig. 9), and 2.7 and 6.1 ml min^{-1} cm^{-3} for larger sponges with numerous oscula studied by Riisgård et al. (1993) and Riisgård et al. (2016), respectively. However, Kumala et al. (2017) measured a mean volume-specific filtration rate of 15 ml min^{-1} cm^{-3} in small single-osculum explants. The reason for up to 5 times difference in value is not clear, but highly variable filtration rates of *H. panicea* haves been found to be a consequence of e.g. changing flow-through that correlated with asynchronous closure of adjacent oscula so that the measured filtration rate reflected a mean value for a sponge consisting of multiple separate modules with open or closed oscula (Riisgård et al. 2016). Thus, the variability of the data used for e.g. power-function scaling may reflect environmentally induced or spontaneous contraction-inflation behavior, including closure and opening of oscula. This sensitivity emphasises that optimal experimental conditions are essential in physiological studies on sponges.

If the volume-specific filtration rate were to depend on size (mean volume of specimens) one would expect it to increase with increasing size as surface area decreases relative to volume holding choanocyte chambers, but this does not seem to be the case. According to our hypothesis that the density of choanocyte pumping units is approximately constant for a given sponge species, this implies that the filtration rate should be a linear function of the sponge volume, which appears to be the case in the present study (Fig. 8) and in the study by Goldstein et al. (2019; Fig. 9). The slope of the regression line in Fig. 9 indicates a volume-specific filtration rate of 3.2 as compared to the 2.3 ml min^{-1} cm^{-3} from the arithmetic mean (Table 1 in Goldstein et al. 2019). Likewise, the slopes in Figs. 8A&B indicate 1.1 and 1.8 ml min^{-1} cm^{-3} as compared to 1.8 and 1.5 ml min^{-1} cm^{-3} from the arithmetic means in Table 1 and Table 3, respectively.

When a single module was exposed locally to ink particles, both the exposed module and its neighbouring modules were triggered to reduce their *OSA* causing pronounced decrease in the filtration rate of the entire multi-oscular explants when compared to undisturbed conditions (Table 3). The underlying mechanism of this form of communication between modules leading to coordinated oscular contractions in the entire multi-oscula sponge may be suggested: sponges have no nerves or muscles, but nevertheless they react to external stimuli in a coordinated way by body contraction and *OSA* reduction because chemical messenger-based systems are involved (Ellwanger et al. 2007; Elliott and Leys 2007, 2010; Tompkins-MacDonald 2008; Pfannkuchen et al. 2009; Nickel et al. 2011; Ludeman et al. 2014; Leys 2015).

Conclusion

The present study shows that a multi-oscula sponge may be regarded as a population of aquiferous modules that share the characteristics of single-osculum explants. Thus, the size of an aquiferous module in a multi-oscula sponge as well as the size of a single-osculum explant is closely correlated with both *OSA* and filtration rate, and the power-function exponents are in fair agreement with the theoretical scaling based on the hypothesis that the density of choanocyte pumping units is constant. In agreement with this suggestion, the filtration rate is a linear function of the sponge volume. Although the individual modules in a multi-oscular sponge operate as separate aquiferous systems, the present study shows that modules nevertheless communicate in response to external stimuli. Specifically, when one module is exposed locally to ink particles, both the exposed module and its neighbouring modules are triggered to reduce their *OSA*.

The underlying mechanism of this form of communication between modules leading to coordinated oscular contractions is suggested to be chemical messenger-based.

Acknowledgements. This work was supported by VILLUM FONDEN under Grant number 9278 and by the Independent Research Fund Denmark under Grant number 8021-00392B.

References

Bagby RM. 1966. The fine structure of myocytes in the sponges *Microciona prolifera* (Ellis and Solander) and *Tedania ignis* (Duchassaing and Michelotti). Journal of Morphology. 118:167−181.

Baty F, Delignette-Muller ML. 2015. Package 'nlstools': tools for nonlinear regression analysis. http://cran.r-project.org/web/packages/nlstools.

Brian CB, Prave AR, Hoffmann KH, Fallick AE, Botha A, Herd DA, Sturrock C, Young I, Condon DJ, Allison SG. 2012. The first animals: ca. 760-million-year-old sponge-like fossils from Namibia. South African Journal of Science. 108:1−8.

Bergquist PR. 1978. Sponges. University of California Press, Berkeley.

Elliott GRD, Leys SP. 2007. Coordinated contractions effectively expel water from the aquiferous system of a freshwater sponge. Journal of Experimental Biology. 210:3736−3748.

Elliott GRD, Leys SP. 2010. Evidence for glutamate, GABA and NO in coordinating behaviour in the sponge, *Ephydatia muelleri* (Demospongiae, Spongillidae). Journal of Experimental Biology. 213:2310−2321.

Ellwanger K, Eich A, Nickel M. 2007. GABA and glutamate specifically induce contractions in the sponge *Tethya wilhelma*. Journal of Comparative Physiology A. 193:1−11.

Ereskovskii AV. 2003. Problems of coloniality, modularity, and individuality in sponges and special features of their morphogeneses during growth and asexual reproduction. Russian Journal of Marine Biology. 29:46−56.

Fox J, Weisberg S, Adler D, Bates D, Baud-Bovy G, Ellison S, Firth D, Friendly M, Gorjanc G, Graves S, Heiberger R. 2012. Package 'car'. R Foundation for Statistical Computing, Vienna, Austria. https://cran.r-project.org/web/packages/car/.

Fry WG. 1970. The sponge as a population: a biometric approach. Symposia of the Zoological Society of London. 25:135−162.

Fry WG. 1979. Taxonomy, the individual and the sponge. Biology and systematics of colonial organisms. Systematics Association, Special. 11:49−80.

Goldstein J, Riisgård HU, Larsen PS. 2019. Exhalant jet speed of single-osculum explants of the demosponge *Halichondria panicea* and basic properties of the sponge-pump. Journal of Experimental Marine Biology and Ecology. 511:82−90.

Jørgensen CB. 1966. Biology of suspension feeding. Pergamon Press, Oxford.

Kumala L, Riisgård HU, Canfield DE. 2017. Osculum dynamics and filtration activity studied in small single-osculum explants of the demosponge *Halichondria panicea*. Marine Ecology Progress Series. 572:117−128.

Larsen PS, Riisgård HU. 1994. The sponge pump. Journal of Theoretical Biology. 168:53−63.

Leys SP. 2015. Elements of a 'nervous system' in sponges. Journal of Experimental Biology. 218:581−591.

Leys SP, Yahel G, Reidenbach MA, Tunnicliffe V, Shavit U, Reiswig HM. 2011. The sponge pump: the role of current induced flow in the design of the sponge body plan. PLoS One 6:1−17.

353 Ludeman DA, Farrar N, Riesgo A, Paps J, Leys SP. 2014. Evolutionary origins of
354 sensation in metazoans: functional evidence for a new sensory organ in sponges.
355 BMC Evolutionary Biology. 14:3. doi:10.1186/1471-2148-14-3
356 Lüskow F, Riisgård HU, Solovyeva V, Brewer JR. 2018. Seasonal changes in bacteria
357 and phytoplankton biomass control the condition index of the
358 demosponge *Halichondria panicea* in temperate Danish waters. Marine Ecology
359 Progress Series (in press).
360 Nickel M. 2004. Kinetics and rhythm of body contractions in the sponge *Tethya*
361 *wilhelma* (Porifera: Demospongiae). Journal of Experimental Biology.
362 207:4515−4524.
363 Nickel M, Donath T, Schweikert M, Beckmann F. 2006. Functional morphology of
364 *Tethya* species (Porifera): 1. Quantitative 3D-analysis of *Tethya wilhelma* by
365 synchrotron radiation based X-ray microtomography. Zoomorphology 125:209−223.
366 Nickel M, Scheer C, Hammel JU, Herzen J, Beckmann F. 2011. The contractile sponge
367 epithelium sensu lato – body contraction of the demosponge *Tethya wilhelma* is
368 mediated by the pinacoderm. Journal of Experimental Biology. 214:1692−1698.
369 Parker GH. 1910. The reactions of sponges, with a consideration of the origin of the
370 nervous system. Journal of Experimental Zoology. 8:1−41.
371 Perovic S, Krasko A, Prokic I, Müller I, Müller WEG. 1999. Origin of neuronal-like
372 receptors in Metazoa: Cloning of a metabotropic glutamate/GABA-like receptor
373 from the marine sponge *Geodia cydonium*. Cell and Tissue Research. 296:395−404.
374 Pfannkuchen M, Fritz GB, Schlesinger S, Bayer K, Brümmer F. 2009. In situ pumping
375 activity of the sponge *Aplysina aerophoba*, Nardo 1886. Journal of Experimental
376 Marine Biology and Ecology. 369:65−71.
377 R Core Team (2015). R: A language and environment for statistical computing. R
378 Foundation for Statistical Computing, Vienna, Austria. http://www.R-project.org/.
379 Reiswig HM. 1971. *In situ* pumping activities of tropical Demospongiae. Marine
380 Biology. 9:38−50.
381 Reiswig HM. 1974. Water transport, respiration and energetics of three tropical marine
382 sponges. Journal of Experimental Marine Biology and Ecology. 14:231−249.
383 Reiswig HM. 1975. The aquiferous systems of three marine Demospongiae. Journal of
384 Morphology. 145:493–502.
385 Riisgård HU, Kumala L, Charitonidou K. 2016. Using the F/R-ratio for an evaluation of
386 the ability of the demosponge *Halichondria panicea* to nourish solely on
387 phytoplankton versus free-living bacteria in the sea. Marine Biology Research.
388 12:907–916.
389 Riisgård HU, Thomassen S, Jakobsen H, Weeks JM, Larsen PS. 1993. Suspension
390 feeding in marine sponges *Halichondria panicea* and *Haliclona urceolus*: effects of
391 temperature on filtration rate and energy cost of pumping. Marine Ecology Progress
392 Series. 96:177–188.
393 Strehlow BW, Jørgensen D, Webster NS, Pineda MC, Duckworth A. 2016. Using a
394 thermistor flowmeter with attached video camera for monitoring sponge excurrent
395 speed and oscular behaviour. PeerJ. 4:e2761. doi:10.7717/peerj.2761.
396 Tompkins-MacDonald GJ, Leys SP. 2008. Glass sponges arrest pumping in response to
397 sediment: implications for the physiology of the hexactinellid conduction system.
398 Marine Biology. 154:973−984.

Table 1. *Halichondria panicea*. Characteristics of 17 single-osculum sponge explants of various size. *D*: osculum diameter; *OSA*: osculum cross-sectional area (Eq. 1); *A*: side-view projected area; *h*: height; V_{est}: estimated explant volume (Eq. 2); U_0: initial exhalant jet speed at distance x = 0 mm from osculum; F_{est}: estimated filtration rate (Eq. 4); $F_v = (F_{est}/V_{est})$: volume specific filtration rate.

ID#	*D* (mm)	*OSA* (mm^2)	*A* (mm^2)	*h* (mm)	V_{est} (cm^3)	U_0 (mm s^{-1})	F_{est} (ml min^{-1})	F_v (ml min^{-1} cm^{-3})
1	0.5	0.2	23.7	3.9	0.15	1.6	0.0	0.00
2	0.5	0.2	37.2	5.6	0.26	10.8	0.1	0.39
3	0.6	0.3	31.1	4.4	0.23	13.1	0.2	0.87
4	0.6	0.3	20.5	2.5	0.18	14.8	0.3	1.70
5	0.6	0.3	16.4	2.8	0.10	12.1	0.2	1.99
6	0.7	0.4	28.4	3.2	0.26	17.7	0.4	1.53
7	0.8	0.6	50.7	7.2	0.38	25.2	0.9	2.40
8	0.9	0.6	34.2	4.6	0.26	10.2	0.4	1.51
9	0.9	0.6	55.7	5.4	0.60	17.7	0.7	1.16
10	0.9	0.7	15.4	2.9	0.90	10.7	0.4	4.63
11	0.9	0.7	53.9	5.4	0.56	12.9	0.5	0.89
12	1.0	0.8	34.0	5.1	0.24	9.4	0.4	1.68
13	1.0	0.8	48.7	5.7	0.44	16.2	0.8	1.83
14	1.1	1.0	49.5	5.2	0.50	14	0.8	1.61
15	1.1	1.0	53.5	6.6	0.45	15.9	1.0	2.20
16	1.2	1.1	45.7	4.9	0.45	19.7	1.3	2.90
17	1.2	1.1	58.6	5.9	0.61	23.9	1.6	2.63
							Mean±S.D.	1.8±1.0

Table 2. *Halichondria panicea.* Hydrodynamic characteristics of a single-osculum sponge explant (V_{est} = 1.0 cm^3) over time. *D*: osculum diameter; *OSA*: osculum cross-sectional area (Eq. 1); U_0: initial exhalant jet speed at distance x = 0 mm from osculum; F_{est}: estimated filtration rate (Eq. 4); F_{mea}: measured filtration rate (clearance method; Fig. 3).

Time (min)	*D* (mm)	*OSA* (mm^2)	U_0 (mm s^{-1})	F_{est} (ml min^{-1})	F_{mea} (ml min^{-1})
0	1.6	1.9	31.1	3.5	
15	1.3	1.4	39.0	3.3	
30	1.4	1.5	33.3	2.9	
45	1.1	0.9	32.2	1.7	
60	1.3	1.4	42.2	3.5	
75	1.1	1.0	41.5	2.5	
90	1.1	0.9	25.7	1.4	
Mean ±SD		1.3 ± 0.3		2.7±0.8	3.6

Table 3. *Halichondria panicea*. Exhalant jet speeds and filtration rates of 6 multi-oscula sponge explants (ID#) prior and post local exposure to ink particles (exposed aquiferous modules marked with **, subsequently affected modules marked with *). O#: osculum number; D: osculum diameter; OSA: osculum cross-sectional area (Eq. 1); U_0: initial exhalant jet speed at distance x = 0 mm from osculum; F_{est}: estimated filtration rate (Eq. 4); V_{mea}: measured volume of the aquiferous module corresponding to each osculum; V_{est}: estimated volume of aquiferous module (Eq. 3); $F_v = (F_{est}/V_{mea})$: volume-specific filtration rate.

ID#	O#	D (mm)	OSA (mm^2)	U_0 (mm s^{-1})	F_{est} (ml min^{-1})	V_{mea} (cm^3)	V_{est} (cm^3)	F_v (ml min^{-1} cm^{-3})
1	1	0.4	0.1	24.4	0.1	0.1	0.1	1.0
	2	0.7	0.4	19.4	0.5	0.3	0.3	1.7
	3	0.8	0.6	33.8	1.2	0.7	0.7	1.7
	4	1.1	1.0	50.6	3.0	1.6	1.7	1.9
				Σ	4.8	2.7	2.8	
1	1*	0.4	0.1	23.4	0.1	-	-	-
	2**	0.4	0.1	11.1	0.1	-	-	-
	3*	0.6	0.3	6.8	0.2	-	-	-
	4*	0.6	0.3	15.3	0.3	-	-	-
				Σ	0.7	-	-	-
2	1	1.6	2.0	50.2	6.0	3.7	3.8	1.6
	2	1.4	1.5	-	-	-	-	-
				Σ	-	-	-	
2	1*	1.5	1.8	60.7	6.5	-	-	-
	2**	1.3	1.4	-	-	-	-	-
				Σ		-	-	
3	1	1.6	1.9	28.0	3.2	1.3	1.2	2.5
	2	2.0	3.1	33.5	6.2	2.3	2.3	2.7
				Σ	9.4	3.6	3.5	-
3	1**	0.6	0.3	0.0	0.0	-	-	-
	2*	0.7	0.3	0.0	0.0	-	-	-
				Σ	0.0	-	-	
4	1	0.7	0.4	14.0	0.3	0.4	0.4	0.8
	2	1.6	1.9	12.4	1.4	1.7	1.8	0.8
				Σ	1.7	2.1	2.2	
4	1**	0.6	0.2	8.6	0.1	-	-	-
	2*	1.4	1.6	13.2	1.3	-	-	-
				Σ	1.4	-	-	
5	1	0.3	0.1	17.3	0.1	0.2	0.2	0.5
	2	0.9	0.6	42.0	1.5	1.1	1.2	1.4
	3	0.6	0.3	57.2	1.0	0.8	0.8	1.3
				Σ	2.6	2.1	2.2	-
5	1*	0.1	0.0	10.2	0.0	-	-	-
	2**	1.1	1.0	28.6	1.7	-	-	-
	3*	0.6	0.3	21.1	0.4	-	-	-
				Σ	2.1	-	-	
6	1	0.4	0.1	3.1	0.3	0.2	0.2	1.5
	2	0.9	0.6	14.5	0.5	0.5	0.6	1.0
				Σ	0.8	0.7	0.8	
6	1*	0.3	0.1	3.5	0.4	-	-	-
	2**	0.9	0.6	16.0	0.6	-	-	-
				Σ	1.0	-	-	
							Mean ± S.D.	1.5±0.6

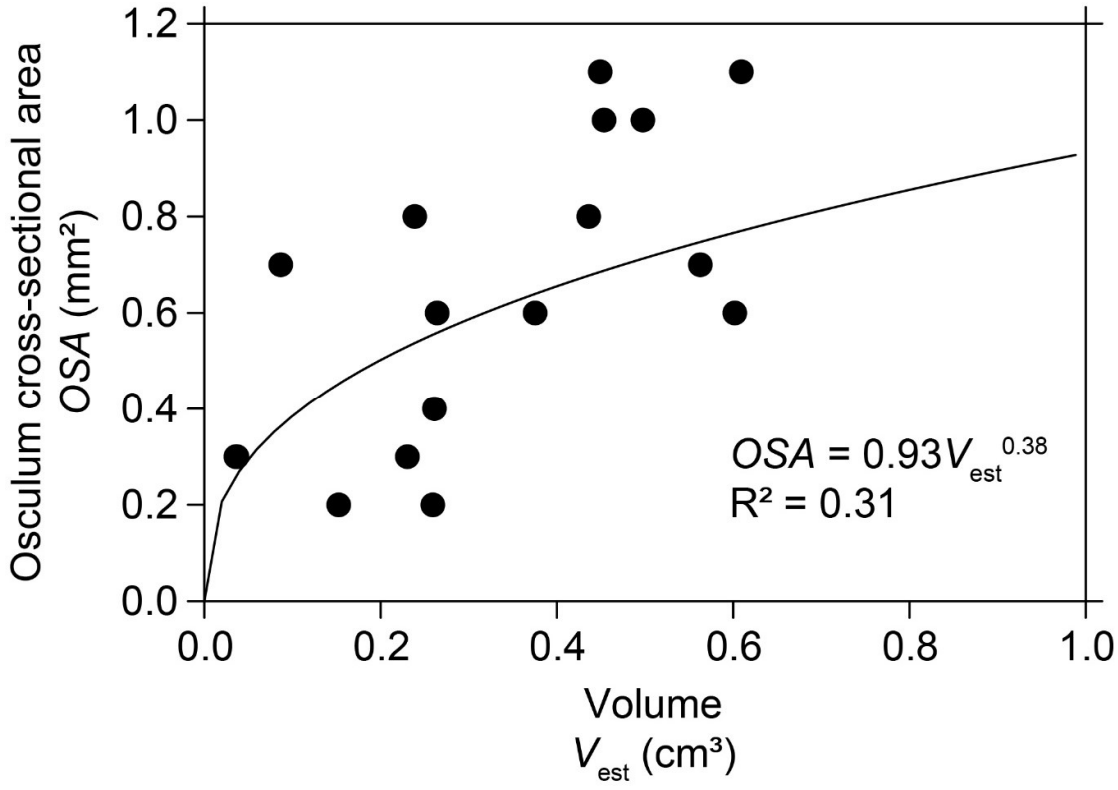

Figure 1. *Halichondria panicea*. Osculum cross-sectional area (*OSA*) as a function of the volume (V_{est}) of a single-osculum sponge explants. Data from Table 1.

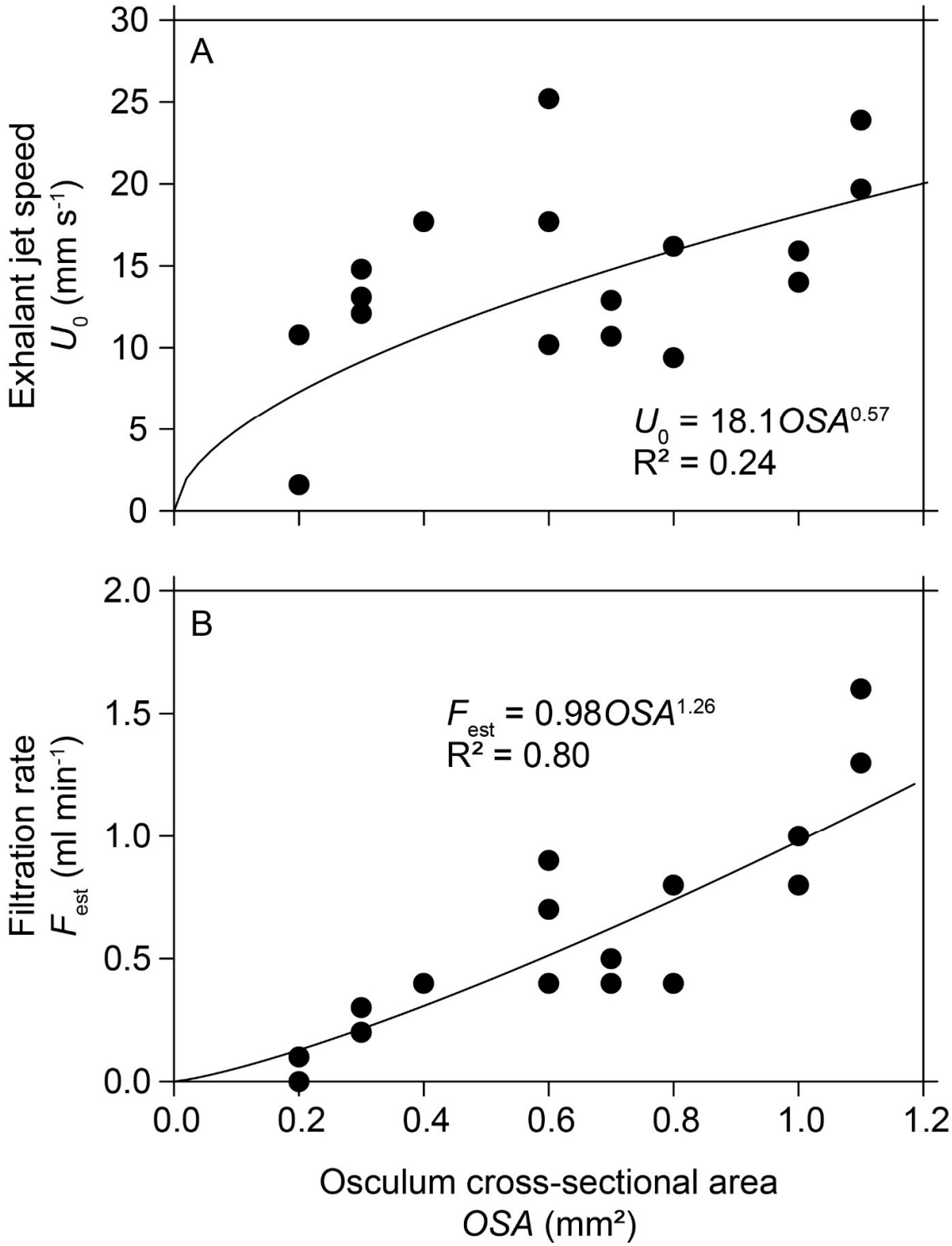

Figure 2. *Halichondria panicea*. (A) Exhalant jet speed (U_0) and (B) estimated filtration rate (F_{est}) as a function of the osculum cross-sectional area (OSA) in single-osculum sponge explants. Data from Table 1.

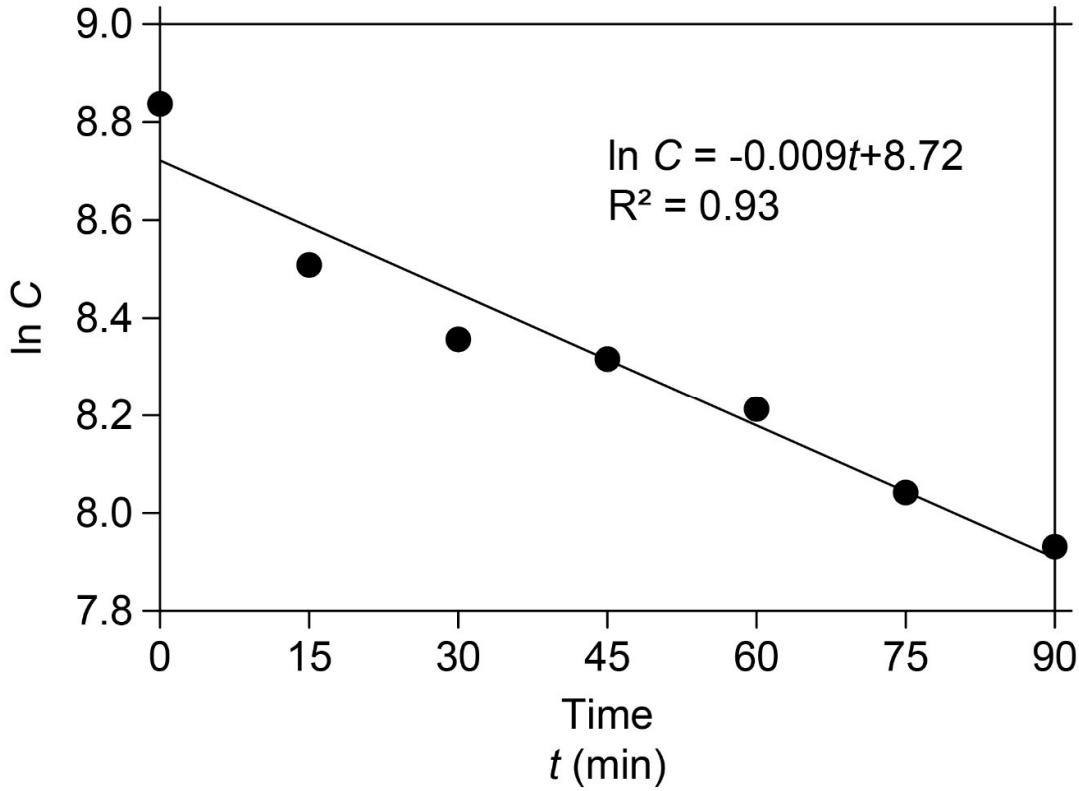

Figure 3. *Halichondria panicea*. Semi-ln plot of reduction in algal (*Rhodomonas salina*) concentration (C, cells ml^{-1}) over time in an aquarium (400 ml) with a single-osculum sponge explant.

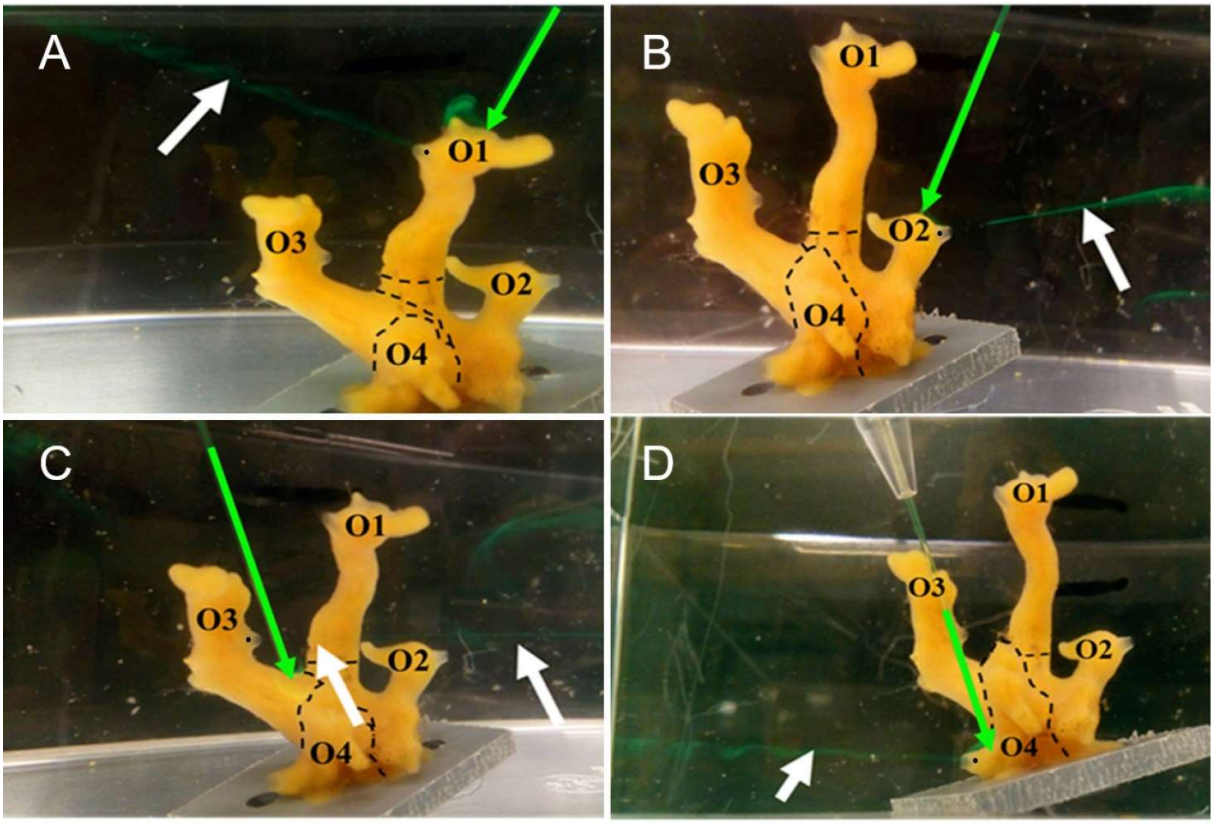

Figure 4. *Halichondria panicea*. Side-view images of exhalant jet indicated by fluorescent dye exiting an osculum indicated by a black dot (A; O1, B; O2, C; O3, D; O4, white arrows) in a four-oscula sponge explant (ID1). Micromanipulator (green arrow) positioned over each aquiferous module (O1, O2, O3, O4). Dashed lines mark boarders mapped between aquiferous modules.

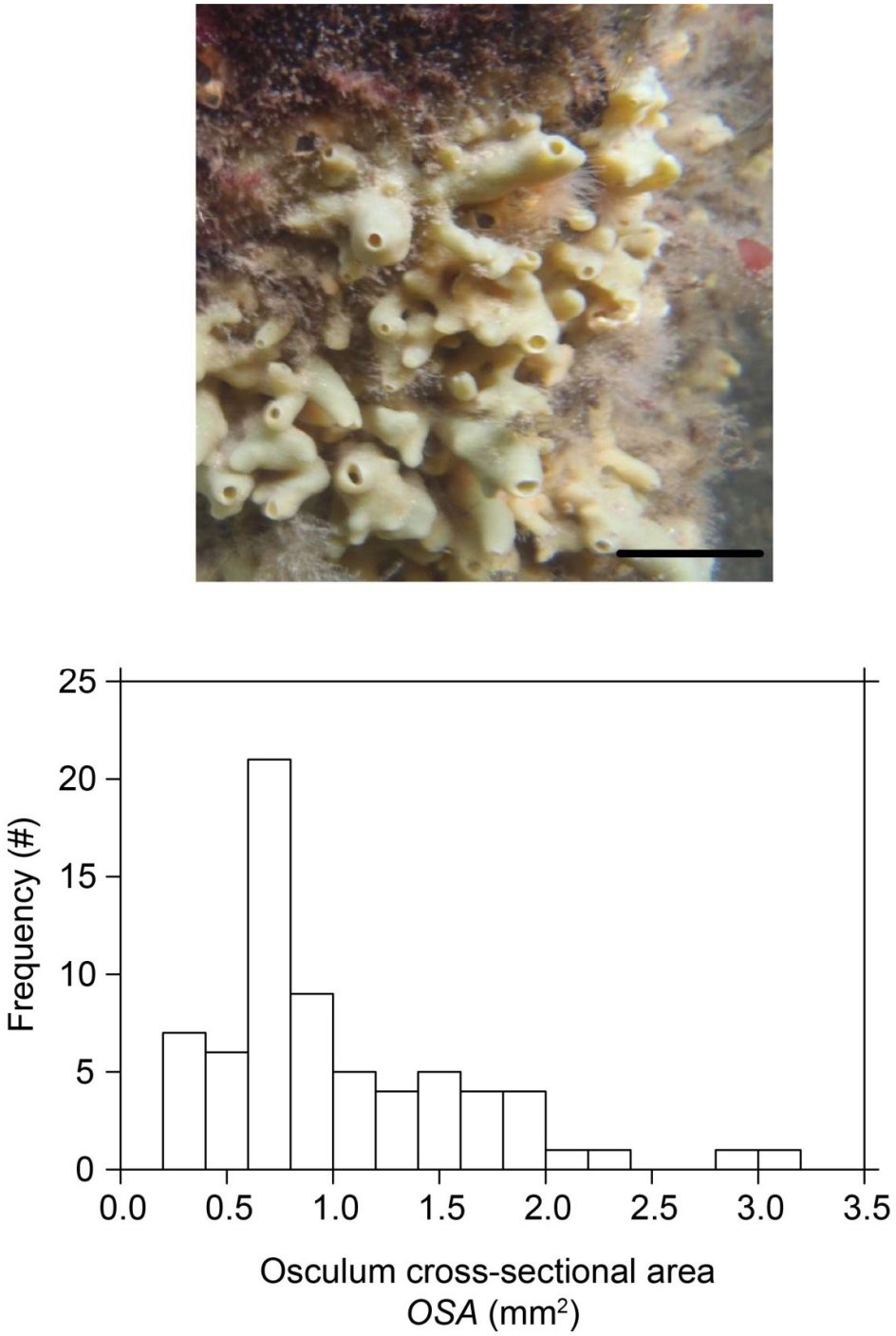

437

438 Figure 5. *Halichondria panicea*. Sponges *in situ* (upper; scale bar: 20 mm) and (lower)
439 *in situ* size distribution of osculum cross-sectional area (*OSA*).

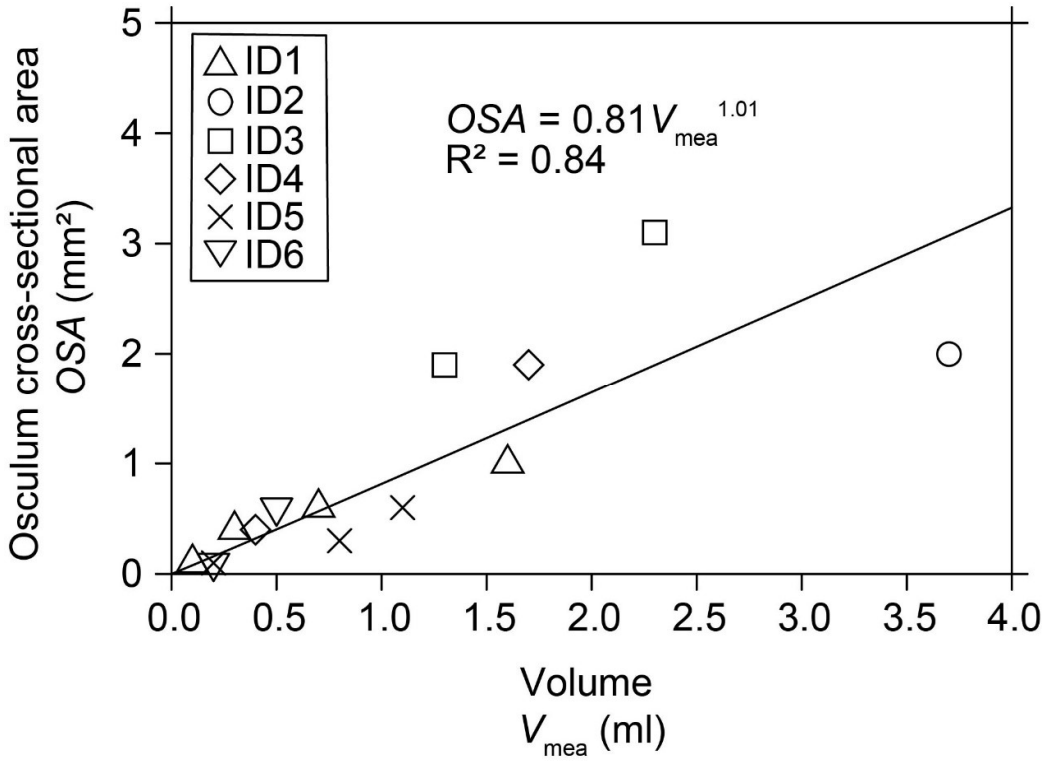

Figure 6. *Halichondria panicea.* Osculum cross-sectional area (*OSA*) as a function of aquiferous module size (V_{mea}) in multi-oscula explants (ID#). Data from Table 3.

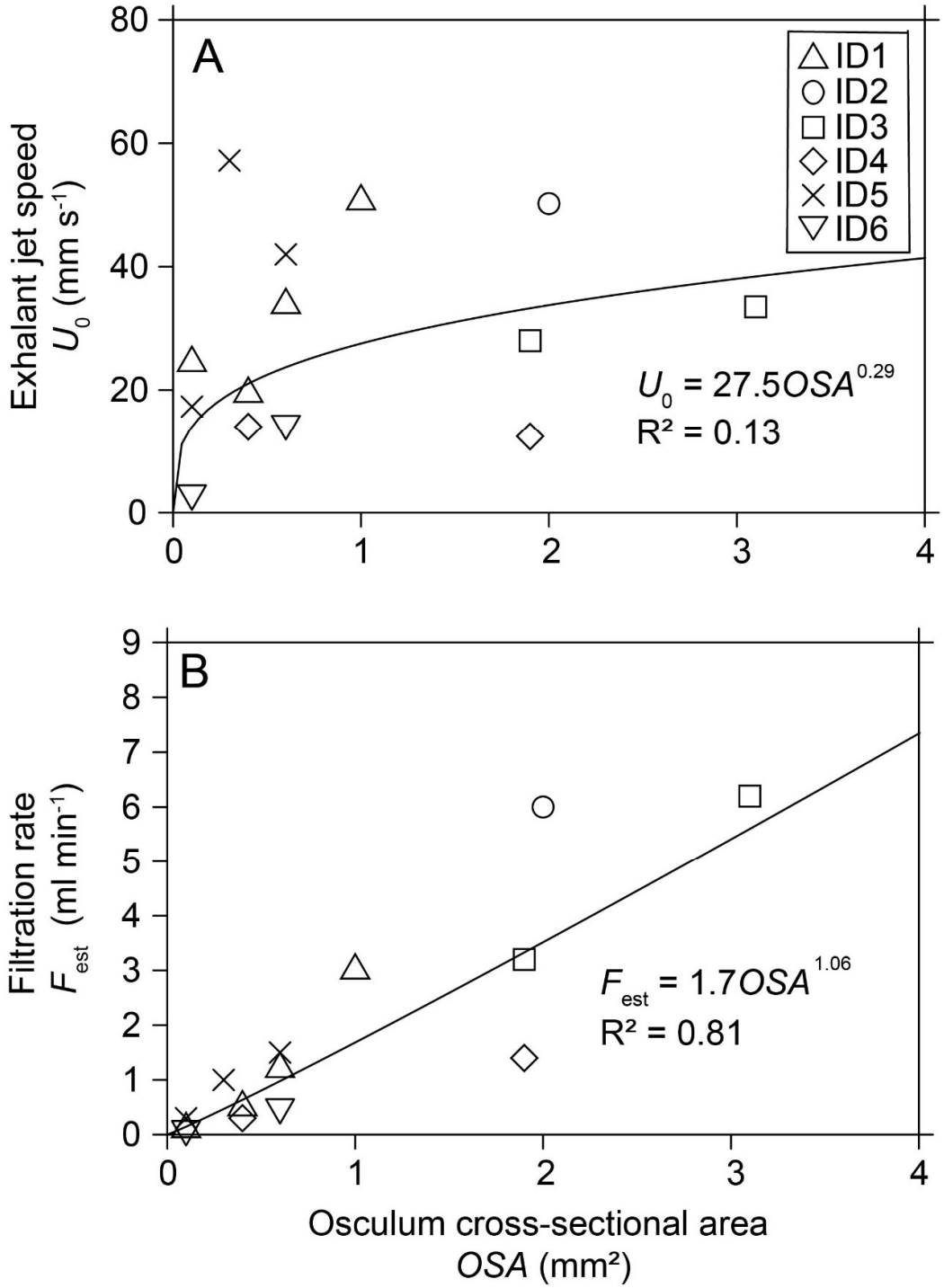

Figure 7. *Halichondria panicea.* (A) Exhalant jet speeds (U_0) and (B) estimated filtration rates (F_{est}) as a function of the osculum cross-sectional area (*OSA)* in aquiferous modules of multi-oscula explants (ID#). Power function of regression line and equation shown. Data from Table 3.

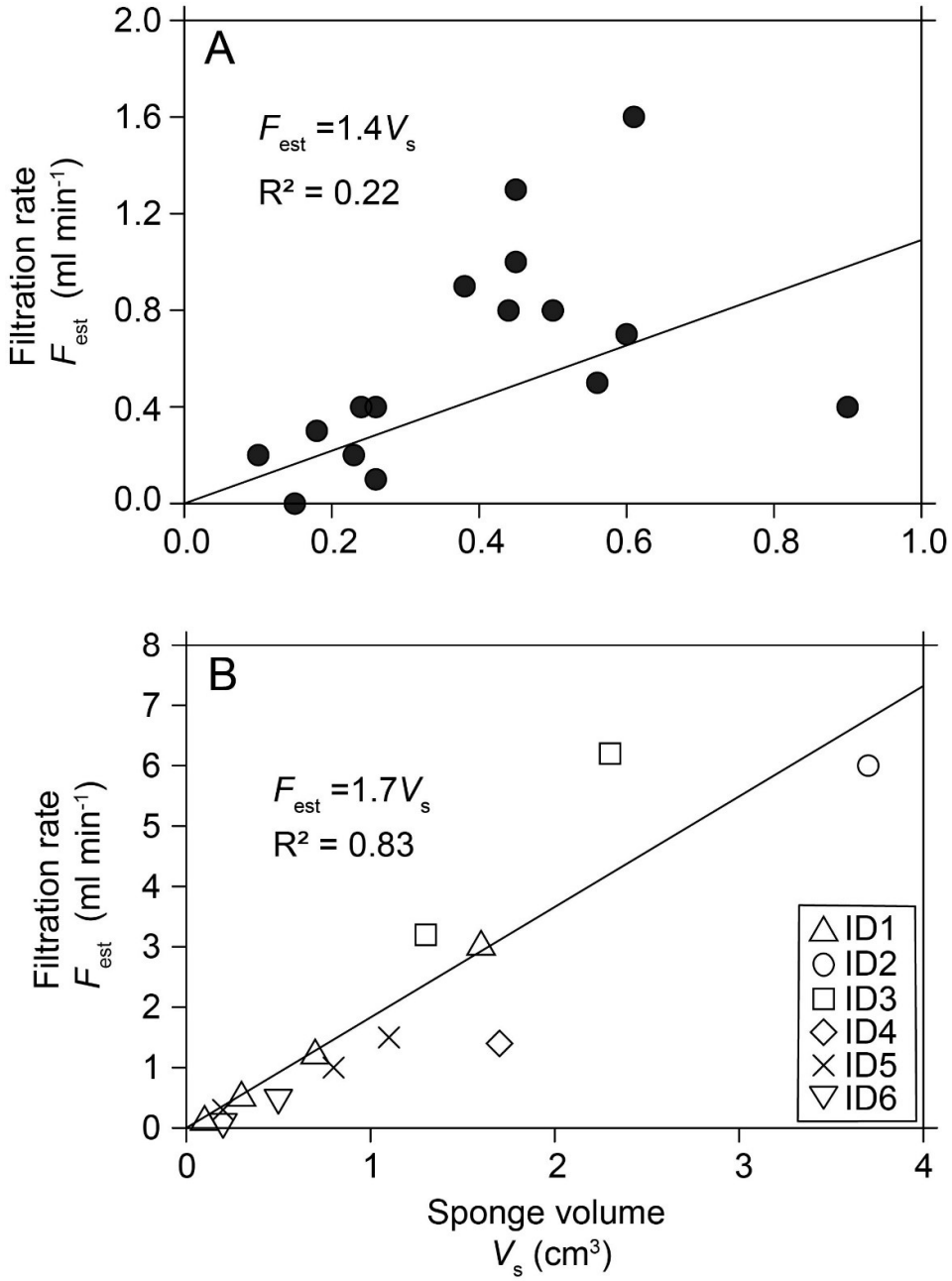

448
449 Figure 8. *Halichondria panicea.* Filtration rate (F_{est}) as a function of aquiferous module
450 size (V_{est}) in single-osculum explants (A, data from Table 1) and multi-oscula explants
451 (ID#) (B, data from Table 3).

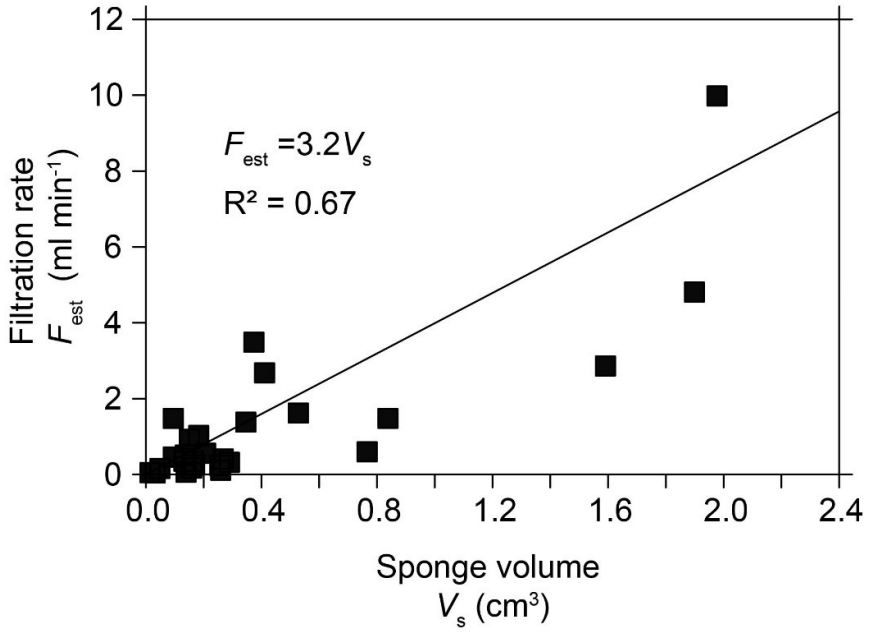

452

453 Figure 9. *Halichondria panicea.* Filtration rate (F_{est}) as a function of aquiferous module
454 size (V_{est}) in single-osculum sponge explants. Data from Goldstein et al. (2019, Table 1
455 therein).